Optics Letters

Radially polarized emission with 635 W of average power and 2.1 mJ of pulse energy generated by an ultrafast thin-disk multipass amplifier

André Loescher,* Jan-Philipp Negel, Thomas Graf, and Marwan Abdou Ahmed

Institut für Strahlwerkzeuge, University of Stuttgart, Pfaffenwaldring 43, 70569 Stuttgart, Germany

**Corresponding author: andre.loescher@ifsw.uni-stuttgart.de*

Received 30 September 2015; revised 7 November 2015; accepted 15 November 2015; posted 16 November 2015 (Doc. ID 251105); published 9 December 2015

We report on a thin-disk multipass amplifier delivering radially polarized laser pulses with an average power of 635 W and 2.1 mJ of pulse energy. To the best of our knowledge, this is the highest average output power and pulse energy reported so far for radially polarized ultrafast lasers. The amplifier is seeded by a TruMicro5050 with 115 W of average output power, 6.5 ps pulse duration, and a repetition rate of 300 kHz. A segmented half-waveplate was used for converting the linearly polarized beam into radial polarization in front of the amplifier. We present a scheme for direct amplification of such doughnut-shaped radially-polarized beams, the results obtained, and a solution to compensate for the depolarizing phase shift introduced by the tilted mirrors in the amplifier.

OCIS codes: (140.3460) Lasers; (140.7090) Ultrafast lasers; (140.3280) Laser amplifiers.

http://dx.doi.org/10.1364/OL.40.005758

Over the last few years, there has been a growing interest in developing laser systems with radial or azimuthal polarization. Due to their axial symmetry, such laser beams show benefits e.g., for material processing. This was first predicted theoretically [1] and later confirmed experimentally for percussion drilling, cutting, and deep-penetration welding [2,3]. Furthermore, a radially polarized beam can be focused more tightly than conventional linearly polarized beams [4]. Laser systems either generate the radial/azimuthal polarization state directly in the resonator or by external conversion of linearly polarized beams by means of different methods (segmented half-waveplate, GIRO mirrors, triple-axicons mirrors, custom-design fibers, etc.) as reported in the literature within the last few years [5–9]. In cw-operation, up to 1.8 kW were extracted from a CO_2 laser with polarization-selective reflector in the resonator [10] and a radially polarized beam with 3 kW of output power was generated by a CO_2 laser with an intracavity circular resonant grating mirror [11]. Using a circular grating inside a thin-disk laser cavity, 275 W of radially polarized radiation at a wavelength of 1030 nm were generated [12]. Single crystal fiber amplifiers for radially/azimuthally polarized beams were demonstrated with up to 100 W of CW average power [13]. In rod lasers, the oscillation in radial or azimuthal polarization significantly reduces depolarization effects and bi-focusing [14]. In this context, 2.1 kW average power with $M^2 < 10$ was demonstrated using Nd:YAG rod amplifiers [15]. Regarding ultrafast laser systems, a very high peak power of 85 GW (at 2 W of average power) was obtained using a Ti:Sa laser system, a segmented waveplate, and a compression stage [16]. In terms of state-of-the-art in average power for ultrafast laser systems, 85 W of average power were recently demonstrated with a multi-stage single-crystal fiber amplifier with pulse duration of 740 fs at 20 MHz repetition rate [17]. Assuming a sech^2-temporal profile, this corresponds to about 5 MW of peak power.

In the present work, we now report on a thin-disk multipass amplifier delivering radially polarized picosecond pulses at an average output power of 635 W and 2.1 mJ of energy per pulse.

The setup of the amplifier is depicted in Fig. 1. The principle of this multipass amplification was first applied to linearly polarized beams and more details of the setup can be found in [18,19]. The main component of the amplifier is the thin-disk laser crystal glued on a diamond heat sink. The disk has a radius of curvature (ROC) of 20.5 m, a thickness of about 130 µm, an at. Yb doping concentration of 10%–11%, and a diameter of 17 mm. It is placed inside a thin-disk module (type G1 as commonly provided by the IFSW). The Trumpf pump diodes deliver up to 2.7 kW of pump power at a wavelength of 969 nm (stabilized by a volume Bragg grating) to exploit the advantages of zero-phonon line pumping [20]. The pump spot on the disk is set to a diameter of about 6–7 mm.

The seed laser system is a TruMicro5050 emitting 6.5 ps long (assuming a Gaussian temporal shape) and linearly polarized laser pulses with a maximum average output power of 115 W. The repetition rate is switchable between 300 and 800 kHz and was set to 300 kHz for the experiments presented here. The beam diameter of the incident beam was 5.5 mm and

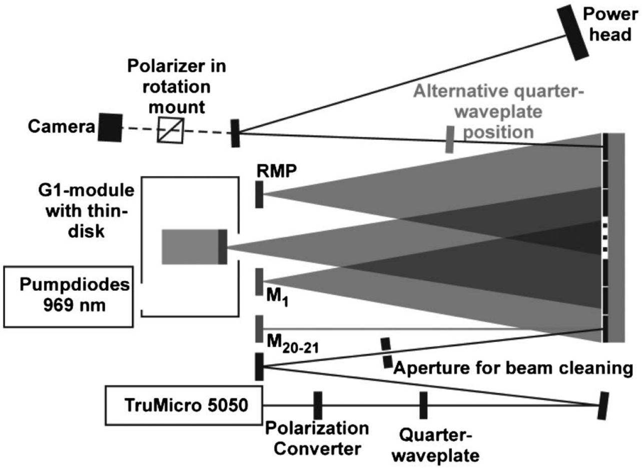

Fig. 1. Schematic overview of the multipass amplifier setup. A TruMicro5050 laser provides the linearly polarized seed beam which is converted into radial polarization by a segmented half-waveplate [2,4,21]. It is injected into the multipass amplifier and follows a propagation path folded by 40 mirrors mounted in an array opposing the thin-disk module [18,19,22]. The beam is reflected 20 times at the laser disk. The quarter-waveplate placed either behind or in front of the amplifier is used to compensate for the depolarizing phase shift introduced by the tilted mirrors of the RMP. Both options were tested during the experiment and led to the same compensation effect. However, as the power is lower at the entrance of the amplifier, we place the quarter-waveplate there for high-power tests to minimize thermal and nonlinear effects. The beam is analyzed using a power head as well as a rotatable polarizer and a camera behind an HR-mirror.

the beam quality factor was measured to be $M^2 = 1.15$. The linear polarization of the seed was converted to radial polarization by means of a polarization converter composed of 8 half-waveplate segments [2,4,21] (we concentrated on radial polarization here while all the results can easily be transferred to azimuthal polarization). The conversion efficiency from the linear Gaussian beam to the radial, doughnut-shaped beam was measured to be larger than 90%, which is very close to the theoretical value of 92% calculated using the software VirtualLab provided by the company LightTrans. This measurement was performed after 5 m of propagation length and behind a beam cleaning aperture to filter the diffracted parts of the beam.

The doughnut-shaped beam is injected into the amplifier and follows a propagation scheme [19] using 40 plane mirrors in an array opposing the thin-disk in a distance of 1170 mm and the three elements M_1, M_{20-21}, and a retroreflecting mirror pair (referred to as "RMP") in a distance of 990, 990, and 920 mm, respectively. The RMP is necessary to overcome limitations by a beam deflection caused by an air wedge in front of the disk introduced by high-power pumping. This beam deflection has a strong impact on dynamic stability of the system [18,19] and is compensated for by the RMP. With this scheme, 20 reflections on the disk can be realized on the present configuration set up for the amplification of radially polarized beams. After leaving the amplifier, the beam is analyzed by measuring the output power as well as observing the beam profile behind an HR turning mirror. Using a polarization analyzer on a rotational mount in front of the camera, the radial polarization state can be analyzed qualitatively. The results of a simulation to calculate the beam diameter along the propagation inside the amplifier assuming a beam quality factor of about $M^2 = 2.3$ is depicted in Fig. 2. This value of 2.3 is based on previous experiments using the same kind of polarization converter. Due to the large ROC of the disk and the doughnut-shaped mode, the beam diameter exhibits only a slight modulation along the propagation, which is very favorable to reduce nonlinearities in the system. The overall propagation length inside the amplifier is about 87 m.

Figure 3 shows the average output power emitted by the multipass amplifier depending on the pump power incident on the thin-disk pumping module for different seed powers. With 115 W of seed power (measured in front of polarization converter and beam cleaning aperture), an average output power of 635 W was obtained at a pump power of 1740 W. With a repetition rate of 300 kHz, this leads to pulse energy of 2.1 mJ. To the best of our knowledge, this is the highest average power and pulse energy demonstrated so far for any ultrafast radially polarized laser. With the seed power being subtracted

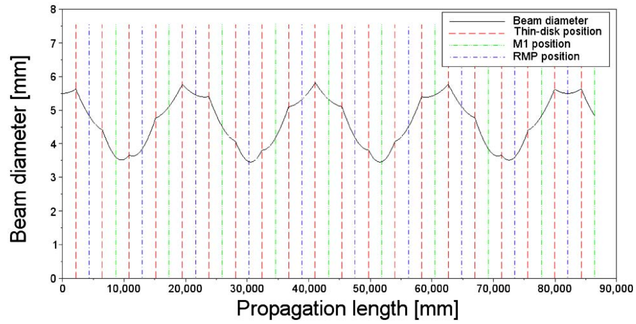

Fig. 2. Beam diameter along the propagation path inside the amplifier. Instead of using a conventional $4f$-propagation scheme, only plane mirrors are used despite the disk with a radius curvature of 20.5 m. In combination with the higher M^2 value of a doughnut-shaped beam, this leads to only a slight modulation of the beam diameter inside the amplifier which is very advantageous to limit nonlinearities.

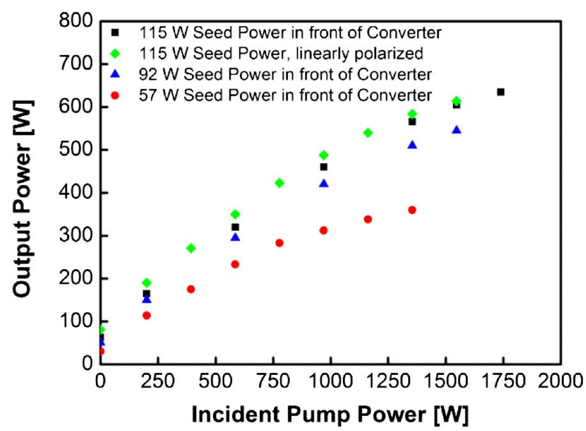

Fig. 3. Output power versus incident pump power for different seed powers. At the highest seed power of 115 W an output power of 635 W was achieved at a pump power of 1740 W. With the seed power being subtracted, this leads to an optical to optical efficiency of about 30%.

the optical to optical efficiency is about 30%. In previous experiments with linear polarization, the pulse duration was measured to be smaller than 8 ps even at 1.4 kW of output power [18]. Therefore, we expect the peak power to be larger than 240 MW (assuming a Gaussian shaped temporal profile).

As expected, lower seed powers lead to smaller extractable output powers, while the amplification factor (ratio between seed power and maximum output power) stays rather constant at a value of about 6. The extractable powers are limited by a "roll-over" in the power slopes which is believed to be due to thermal effects on the disk [18]. This roll-over can be mitigated in a future setup by using more passes over the disk.

The doughnut-shaped mode exhibits a vanishing intensity in the center of the intensity profile while the pumping distribution in the thin-disk laser crystal has a super-Gaussian shape. Therefore, one could assume that there is less extraction of the stored energy in the center of the disk which is causing thermal problems. However, it was found that a Gaussian-shaped linearly polarized beam and the doughnut-shaped radially polarized beam lead to almost the same extractable output power (see Fig. 3). We believe that this can be explained by a slight change of the position of the different seed beam passes on the disk at high-power pumping, leading to a power extraction also in the center of the pumped region of the thin-disk crystal. Furthermore, the overlap integral of either the Gaussian beam with the super-Gaussian pumping distribution is slightly lower than the one of the doughnut-shaped beam with the same pumping distribution.

Along the propagation and through the amplifier, the laser beam passes the RMP after every second pass over the disk. The RMP consists of two mirrors mounted at an angle of incidence of 45 deg. Since there is a phase-shift between the *s*- and *p*-polarization components at every reflection on the tilted mirrors, the multiple passes on the RMP lead to depolarization which can be quantitatively expressed by the reduction of the Degree Of Radial Polarization (DORP) or radiality [23]. By nature, no depolarization occurs in the sagittal and tangential planes because there the incident field is either purely *s*- or *p*-polarized. In the beam's cross section, the highest depolarizing impact is found at the axes at an azimuthal angle of 45 deg with respect to the sagittal and tangential planes. We have calculated the resulting DORP depending on the number of reflections on the disk using an extended Jones-Matrix-Formalism [23], see Fig. 4. For the sake of simplicity, it was assumed that there is one tilted RMP mirror after every pass through the laser disk rather than two after every second pass. The phase shift between *s*- and *p*-polarized radiation, which mainly occurs at the reflection of the tilted RMP mirror, was determined from a measurement with a polarimeter setup and a probe beam with linear polarization oriented by 45 deg with respect to the sagittal and tangential planes. It was found that on average the total phase shift in one single path, including the reflections on the thin-disk crystal and on one RMP mirror, sums up to about 12.5 deg. Starting with a pure radially polarized transverse mode, a phase shift between *s*- and *p*-polarization at the tilted mirrors leads to a gradual transition to a hybrid mode with radial polarization in the sagittal and tangential directions and azimuthal polarization in the directions at the 45 deg between these planes. According to the definition, the value of the DORP is reduced to 0% when the original radially polarized mode is completely converted into

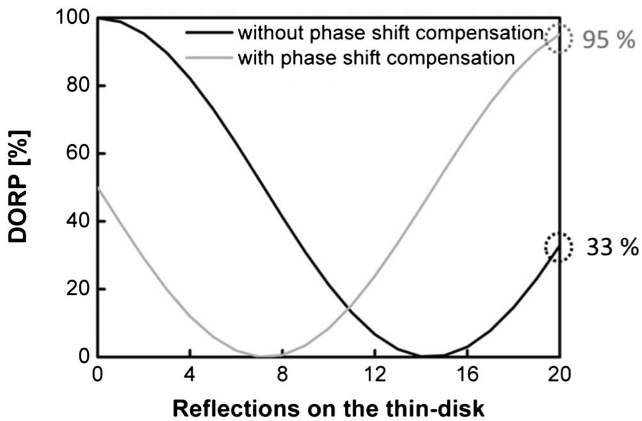

Fig. 4. Calculated DORP [23] as a function of the number of passes on the thin-disk crystal assuming a phase shift of 12.5 deg between *s*- and *p*-polarization occurring at one bounce on a 45-deg mirror per disk pass (black). Same calculation with a quarter-waveplate added at the beginning of the propagation (gray) with its fast axis oriented at an angle of 135 deg with respect to the sagittal plane at the tilted RMP mirror. This allows for a very good compensation for the depolarization introduced by the phase-shift at the tilted dielectric mirrors.

this hybrid mode. With the measured 12.5 deg of phase shift per single pass, it follows from the simulation that after 20 passes the DORP is reduced to about 33%. This was qualitatively verified in the experiment. Figure 5(a) shows the doughnut-shaped beam profile observed by a camera behind an HR mirror after the beam leaves the amplifier. Figure 5(b) shows the image with a polarizer mounted on a rotation stage in front of the camera when the amplifier was operated at an average output power of about 600 W. For the orientations of 0 and 90 deg of the polarizer (corresponding to the sagittal and the tangential planes at the tilted mirrors of the RMP, respectively), the two lobes are separated as expected for a radially polarized beam. Differences in intensities in these pictures are most probably due to small differences in the transmission characteristics of the HR mirror for *s*- and *p*-polarization. Without corresponding compensation, the phase shift introduced by the tilted mirrors leads to a strong distortion of the polarization state and the lobes measured at the diagonal axes of 45 and 135 deg are not separated any more.

To overcome these limitations, an effective compensation method was introduced. As shown by Fig. 4, the depolarization caused by the phase shift on the tilted mirrors can very effectively be compensated for by inserting a quarter-wave plate in front of or at the exit of the amplifier. The fast axis of the quarter-wave plate is oriented at an angle of 135 deg with respect to sagittal plane at the tilted mirrors of the RMP. With this, the periodic modulation of the DORP is shifted, but at the expense of a slight decrease of the maximum value. In the present setup, the calculations predict that it is possible to reach a DORP of about 95% with the help of the quarter-waveplate.

This compensation scheme was verified experimentally by positioning the quarter-waveplate in front of the amplifier since there is less power propagating through the element in comparison to the position at the exit of the amplifier. The insertion of the quarter-waveplate had no influence on the resulting output power. The analysis of the resulting polarization distribution, measured at an output power of 635 W, is shown in

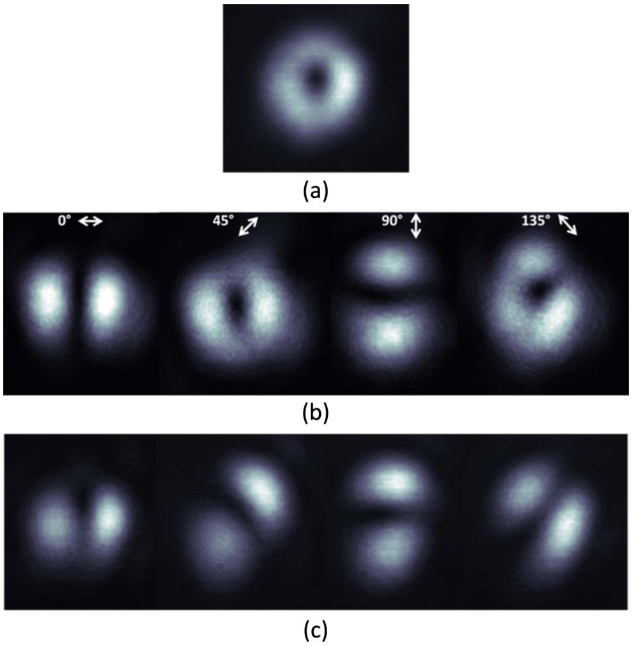

Fig. 5. Intensity distributions of the beam profile recorded to analyze the polarization distribution. (a) Without the polarizer the output beam shows its typical doughnut-shaped mode. (b) Without the quarter-waveplate in the beam path, depolarization caused by the phase shift introduced by the tilted mirrors can be observed by rotating the analyzing polarizer to 45 and 135 deg. (c) With the quarter-waveplate in front of the amplifier very good phase shift compensation can be achieved and the depolarizing effect is minimized.

Fig. 5(c). The detected lobes are now well separated for all rotation angles (0, 45, 90, and 135 deg) of the polarizer, which confirms that the depolarization effect introduced by the tilted mirrors can well be compensated for by the inserted quarter-waveplate. Furthermore, no differences were observed at different power levels, which indicates that the thermally loaded thin-disk laser crystal does not introduce significant additional depolarization.

In summary, we demonstrated a thin-disk multipass amplifier for radially polarized laser pulses with an average output power of 635 W, 2.1 mJ of energy per pulse, and an expected peak power of more than 240 MW. To the best of our knowledge, this is the highest average output power and highest pulse energy demonstrated so far for an ultrafast radially polarized laser. Furthermore, high radial polarization purity was achieved by introducing a quarter-waveplate to compensate for the phase shifts occurring at the tilted mirrors in the amplifier. The DORP of a beam with phase shift compensation was measured in a similar system to be around 94%. However, higher DORP is achievable by optimizing the applied phase-shift compensation.

Future experiments will be devoted to further power scaling by increasing the number of passes over the disk and to the amplification of shorter pulses in the fs-regime. Additionally, other compensation techniques which allow for an even higher DORP will be investigated. This is especially suitable for pre-compensation of phase shifts in material processing experiments that are using 45 deg turning mirrors.

Funding. European Union Seventh Framework Programme [FP7/20072013] (619237); German Federal Ministry of Education and Research (BMBF) (13N11787).

Acknowledgment. We would like to thank Trumpf Laser GmbH for providing the TruMicro5050 seed source and the VBG-stabilized pump diodes.

REFERENCES

1. V. G. Niziev and A. V. Nesterov, J. Phys. D **32**, 1455 (1999).
2. M. Kraus, M. Abdou-Ahmed, A. Michalowski, A. Voss, R. Weber, and T. Graf, Opt. Express **18**, 22305 (2010).
3. R. Weber, A. Michalowski, M. Abdou-Ahmed, V. Onuseit, V. Rominger, M. Kraus, and T. Graf, Phys. Procedia **12**, 21 (2011).
4. R. Dorn, S. Quabis, and G. Leuchs, Phys. Rev. Lett. **91**, 233901 (2003).
5. S. Ramachandran, P. Kristensen, and M. F. Yan, Opt. Lett. **34**, 2525 (2009).
6. M. Endo, Opt. Lett. **33**, 1771 (2008).
7. T. Moser, J. Balmer, D. Delbeke, P. Muys, S. Verstuyft, and R. Baets, Appl. Opt. **45**, 8517 (2006).
8. D. Lin and W. A. Clarkson, Opt. Lett. **40**, 498 (2015).
9. T. Kämpfe, S. Tonchev, A. V. Tishchenko, D. Gergov, and O. Parriaux, Opt. Express **20**, 5392 (2012).
10. A. Nesterov, V. Niziev, and V. Yakunin, J. Phys. D **32**, 2871 (1999).
11. M. Abdou-Ahmed, J. Schulz, A. Voss, O. Parriaux, J. Pommier, and T. Graf, Opt. Lett. **32**, 1824 (2007).
12. M. Abdou-Ahmed, M. Haefner, M. Vogel, C. Pruss, A. Voss, W. Osten, and T. Graf, Opt. Express **19**, 5093 (2011).
13. S. Piehler, X. Délen, M. Rumpel, J. Didierjean, N. Aubry, T. Graf, F. Balembois, P. Georges, and M. A. Ahmed, Opt. Express **21**, 11376 (2013).
14. T. Moser, M. Abdou-Ahmed, F. Pigeon, O. Parriaux, E. Wyss, and T. Graf, Laser Phys. Lett. **1**, 234 (2004).
15. I. Moshe, S. Jackel, A. Meir, Y. Lumer, and E. Leibush, Opt. Lett. **32**, 47 (2007).
16. S. Carbajo, E. Granados, D. Schimpf, A. Sell, K. Hong, J. Moses, and F. X. Kärtner, Opt. Lett. **39**, 2487 (2014).
17. F. Lesparre, J. Gomes, X. Délen, I. Martial, J. Didierjean, W. Pallmann, B. Resan, M. Eckerle, T. Graf, M. Abdou-Ahmed, F. Druon, F. Balembois, and P. Georges, Opt. Lett. **40**, 2517 (2015).
18. J. Negel, A. Loescher, A. Voss, D. Bauer, D. Sutter, A. Killi, M. A. Ahmed, and T. Graf, Opt. Express **23**, 21064 (2015).
19. J. Negel, A. Voss, D. Bauer, D. Sutter, A. Killi, M. A. Ahmed, and T. Graf, Opt. Lett. **38**, 5442 (2013).
20. B. Weichelt, A. Voss, M. A. Ahmed, and T. Graf, Opt. Lett. **37**, 3045 (2012).
21. G. Machavariani, Y. Lumer, I. Moshe, A. Meir, and S. Jackel, Opt. Lett. **32**, 1468 (2007).
22. A. Antognini, K. Schuhmann, F. D. Amaro, F. Biraben, A. Dax, A. Giesen, T. Graf, T. W. Hänsch, P. Indelicato, L. Julien, C.-Y. Kao, P. E. Knowles, F. Kottmann, E. L. Bigot, Y.-W. Liu, L. Ludhova, N. Moschüring, F. Mulhauser, T. Nebel, F. Nez, P. Rabinowitz, C. Schwob, D. Taqqu, and R. Pohl, IEEE J. Quantum Electron. **45**, 993 (2009).
23. A. Voss, M. A. Ahmed, and T. Graf, Opt. Express **18**, 21540 (2010).